Atmos. Chem. Phys. Discuss., 10, 18063–18099, 2010
www.atmos-chem-phys-discuss.net/10/18063/2010/
doi:10.5194/acpd-10-18063-2010

Atmospheric Chemistry and Physics Discussions

Evidence for heterogeneous chlorine activation in the tropical UTLS

M. von Hobe[1], J.-U. Grooß[1], G. Günther[1], P. Konopka[1], I. Gensch[1], M. Krämer[1], N. Spelten[1], A. Afchine[1], C. Schiller[1], A. Ulanovsky[2], N. Sitnikov[2], G. Shur[2], V. Yushkov[2], F. Ravegnani[3], F. Cairo[3], A. Roiger[4], C. Voigt[4], H. Schlager[4], R. Weigel[5], W. Frey[5], S. Borrmann[5], R. Müller[1], and F. Stroh[1]

[1]Forschungszentrum Jülich GmbH, Institute for Chemistry and Dynamics of the Geosphere ICG-1: Stratosphere, Jülich, Germany
[2]Central Aerological Observatory, Dolgoprudny, Moscow, Russia
[3]Institute of Atmospheric Sciences and Climate CNR-ISAC, Bologna, Italy
[4]Deutsches Zentrum für Luft und Raumfahrt, Institut für Physik der Atmosphäre, Oberpfaffenhofen, Germany
[5]Johannes Gutenberg Universität Mainz, Institute of Atmospheric Physics, Mainz, Germany

Received: 2 June 2010 – Accepted: 13 July 2010 – Published: 29 July 2010

Correspondence to: M. von Hobe (m.von.hobe@fz-juelich.de)

Published by Copernicus Publications on behalf of the European Geosciences Union.

Abstract

Airborne in-situ observations of ClO in the tropics were made during the TROCCINOX (Aracatuba, Brasil, February 2005) and SCOUT-O_3 (Darwin, Australia, November/December 2005) field campaigns. While during most flights significant amounts of ClO (≈10–20 parts per trillion, ppt) were present only in aged stratospheric air, instances of enhanced ClO mixing ratios of up to 40 ppt – significantly exceeding those expected from gas phase chemistry – were observed in air masses of a more tropospheric character. Most of these observations concur with low temperatures or with the presence of cirrus clouds (often both), suggesting that cirrus ice particles and/or liquid aerosol at low temperatures may promote significant heterogeneous chlorine activation in the tropical upper troposphere lower stratosphere (UTLS). In two case studies, particularly high levels of ClO observed were reproduced by chemistry simulations only under the assumption that significant denoxification had occurred in the observed air. At least for one of these flights, a significant denoxification is in contrast to the observed NO levels suggesting that the coupling of chlorine and nitrogen compounds in the tropical UTLS may not be completely understood.

1 Introduction

Ozone trends in the tropopause region play an important role in the radiative forcing of the Earth's climate system (Ramaswamy et al., 2001). The causes for decreasing ozone trends in this region over the 1980s and 1990s have not yet been fully understood (WMO, 2006; Logan, 1999). While changes in transport in the lowermost stratosphere could explain at least part of the observed trend (Fusco and Salby, 1999; Salby and Callaghan, 2004; Hood and Soukharev, 2005), chemical ozone loss due to halogen chemistry is also thought to play a significant role (Salawitch et al., 2005; Solomon et al., 1997). Besides higher than previously suggested and still slightly increasing amounts of bromine in this region (Dorf et al., 2006), catalytic ozone destruction by ClO produced as a result of heterogeneous chlorine activation on sulphate aerosol and on ice-particles in cirrus clouds has been suggested (Borrmann et al., 1996; Borrmann et al., 1997; Bregman et al., 2002; Keim et al., 1996; Solomon et al., 1997; Thornton et al., 2003, 2005).

Known reactions by which chlorine can be heterogeneously activated are

$$HCl + ClONO_2 \rightarrow Cl_2 + HNO_3 \qquad \text{(R1)}$$

$$HCl + HOCl \rightarrow Cl_2 + H_2O \qquad \text{(R2)}$$

$$H_2O + ClONO_2 \rightarrow HOCl + HNO_3 \qquad \text{(R3)}$$

$$HCl + HOBr \rightarrow H_2O + BrCl \qquad \text{(R4)}$$

Reaction (R1) was first suggested by Solomon et al. (1986) as a key process leading to the activation of the main chlorine reservoir species HCl and $ClONO_2$ and subsequent rapid ozone destruction in the Antarctic stratosphere in winter. This suggestion prompted numerous laboratory studies and the discovery of a number of further heterogeneous reactions of importance to stratospheric chemistry (e.g. Reactions R2–R4). Today, the reaction rates of heterogeneous reactions on a variety of surfaces are reasonably well constrained through laboratory studies (Sander et al., 2006). While polar stratospheric clouds (PSCs) occur in stratospheric air containing significant amounts of chlorine reservoir species (in the parts per billion, ppb range), the situation near the tropopause is different. Tropospheric aerosol number densities decrease sharply with altitude and water vapour saturation leading to cirrus formation is most likely to be found in humid tropospheric air masses, while sizeable amounts of inorganic chlorine (Cl_y=HCl+$ClONO_2$+Cl+ClO+2 ClOOCl+OClO+HOCl) are present only in photochemically aged air masses of stratospheric origin, which on average are comparatively dry. Thus it has been pointed out that heterogeneous chlorine activation plays a significant role only in regions where wet tropospheric air masses are mixed with stratospheric air (Solomon et al., 1997). While at mid and high latitudes, air with a significant stratospheric signature (characterised by high abundance of ozone) is often found below the thermal tropopause due to downward transport, the Cl_y content inside high altitude cirrus clouds coupled to local deep convection is generally low, and significant amounts of Cl_y to be activated are present only at the interface between the cloud and stratospheric air at the top of the cloud (Solomon et al., 1997).

Cirrus clouds extending up to or above the tropopause are most likely to be found in mid-latitudes (45 to 65°) and in the inner tropics (Wang et al., 1996). The altitude of the tropopause in these regions is very different: typically 10 to 12 km in mid latitudes and 15 to 17 km in the tropics. Tropical Cirrus clouds are particularly widespread and often optically thin (Wang et al., 1996). For mid and high latitudes a number of observations of ClO near the tropopause exists and has been linked to heterogeneous activation on cirrus or background aerosol (Thornton et al., 2003; Borrmann et al., 1997; Keim et al., 1996; Stroh et al., 2004). Here we present observations of ClO from the TROCCINOX (Tropical Convection, Cirrus, and Nitrogen Oxides Experiment) and the SCOUT-O_3 (Stratospheric-Climate Links with Emphasis on the Upper Troposphere and Lower Stratosphere) aircraft campaigns, which represent the first in-situ measurements of enhanced ClO in the upper troposphere and lower stratosphere (UTLS) in the tropics. In Sect. 3.1, we show that in some cases the observed ClO mixing ratios cannot be explained by gas phase chemistry alone, but are likely to be caused by heterogeneous reactions on cold sulphate aerosol or on cirrus ice particles. In particular, we investigate events of concurrent or preceding cirrus cloud formation both below the tropopause (TROCCINOX) and extending into the lowermost stratosphere (SCOUT-O_3). The parameters that are most likely to influence the extent of heterogeneous chlorine activation are investigated (Sect. 3.2), and case studies for incidences of unusually high ClO are presented, where observations are compared to model simulations of heterogeneous activation and chemical deactivation of active chlorine (Sect. 4).

2 Experiment

2.1 Field observations

Observations were made during two field campaigns with the super–high–altitude research aircraft M55-Geophysica. In February 2005, the aircraft was deployed from Araçatuba, Brazil, during the TROCCINOX campaign. Observations inside cirrus clouds were made during several flights in the altitude range 10–15 km (see Huntrieser et al., 2007, and Konopka et al., 2007, for detailed information on all flights and meteorological conditions). During the SCOUT-O_3 campaign in November/December 2005, flights were carried out from Darwin, Australia. Convective storms reaching altitudes of up to 20 km were observed, and cirrus clouds were found above the tropopause at altitudes as high as 17 km (for information on flights and meteorology see Brunner et al., 2009).

Chlorine monoxide (ClO) was measured by the HALOX instrument situated in a pod underneath the left wing of the Geophysica aircraft (von Hobe et al., 2005). It employs the chemical conversion resonance fluorescence (CCRF) technique described by Brune et al. (1989). Through an inlet optimised for radical measurements, ambient air is pulled through two measurement ducts where periodically (10 or 20 s cycles) NO is added converting ClO to chlorine atoms that are detected downstream by resonance fluorescence in the vacuum UV. Accuracy is estimated to be ≈16%, resulting from uncertainties in the Cl atom VUV (118.9 nm) absorption coefficient (Schwab and Anderson, 1982), the scattering characteristics of the RF cell, the contribution of the Lyman-α spectral line to the lamp output, and the ClO to Cl chemical conversion efficiency. More critical for the analysis presented below is precision, which is influenced largely by the output and stability of the chlorine emission lamps and the detector noise observed. These parameters varied during both campaigns and were generally better during TROCCINOX. The signal-to-noise-ratio can be increased by integrating the signal over several NO addition cycles, resulting in a better precision at the expense of time resolution. For the data presented here, the number of cycles averaged was determined for each flight – and in some cases flight segment – individually so that mixing ratios in the range of only a few ppt present in the tropical UTLS could be detected with reasonable precision (ranging from ≈10 to 50%) and a time resolution (2–10 min during TROCCINOX and 1 to 30 min during SCOUT-O_3) in the same order as individual cirrus events observed by other instruments.

Ozone measurements were performed by the FOZAN-II (Fast Ozone Analyzer) instrument jointly developed and operated by the Central Aerological Observatory, Russia, and Institute of Atmospheric Science and Climate, Italy (Ulanovsky et al., 2001; Yushkov et al., 1999). It has two channels with solid state chemiluminescent sensors and measures ozone in the concentration range of 10–500 g/m^3 with a time resolution of 1 s and a precision of <10% at ambient pressures between 30 and 1000 hPa. FOZAN is equipped with a high accuracy ozone generator for periodical calibration of each channel every 15 min.

NO_y and NO were determined by the SIOUX (Stratospheric observation unit for nitrogen oxides) instrument. SIOUX includes two channels for detection of nitric oxides (NO), total reactive nitrogen (NO_y), and NO_y contained in particles larger than about 1 µm in diameter (Schmitt, 2003; Voigt et al., 2005). The detection of NO is based on NO/O_3-chemiluminescence. Higher oxidized NO_y species are reduced to NO using a heated Au converter and CO gas as catalyst. Particle-phase NO_y is detected by oversampling of particles in a forward facing subisocinetic inlet and evaporation and reduction of condensed NO_y in the heated inlet and Au converter (Voigt et al., 2007). The nominal accuracy and precision of the gas-phase measurements are 10%/5% (NO) and 15%/7% (NO_y).

Evidence for cirrus clouds and potential recent heterogeneous processing is gathered from observations of water vapour and particles. Total water, i.e. gas phase and condensed phase, was determined with a measurement frequency of 1 s^{-1} by the Fast In situ Stratospheric Hygrometer (FISH) based on the Lyman-α photofragment fluorescence technique. Details of the instrument and the calibration procedure are described in Zöger et al. (1999). To detect and quantify water in the condensed phase, the saturation water vapour at the given pressure and temperature was subtracted from the total water (Schiller et al., 2008). The FISH measurements made during the TROCCINOX and SCOUT-O_3 campaigns have recently been published by Schiller et al. (2009).

In addition, gas phase water vapour was determined by the Fluorescent Airborne Stratospheric Hygrometer (FLASH) developed in Central Aerological Observatory (Sitnikov et al., 2007). As FISH instrument it is based on Lyman-α photofragment fluorescence method. Special construction of inlet permits to avoid the influence of condensed water phase.

Further evidence for the presence and nature of particles is obtained from the Multiwavelength Aerosol Scatterometer (MAS) (Buontempo et al., 2006) observations of volume depolarisation at 532 nm. MAS is a laser backscatter sonde measuring in situ aerosol optical parameters, by revealing cross and direct polarisation backscattered light at different wavelengths. During daytime, only the 532 nm Nd-YAG-diode pumped laser has sufficient energy to detect the backscattered signal.

Aerosol number densities in the size range from 6 nm up to 1 µm particle diameter were measured by the Condensation Particle Counting System (COPAS) (Weigel et al., 2009) consisting of an aerosol inlet and two dual-channel continuous flow Condensation Particle Counters (CPCs). Three channels are operated with distinct temperature differences between the saturator and the condenser block yielding smallest detectable particle sizes of 6 nm, 11 nm, and 15 nm, respectively, at ambient pressure of 70 hPa. The fourth channel is operated with an aerosol heating line for a determination of the non-volatile number of particles.

Cloud particles in the size range 2.7 and 31 µm diameter were measured using a Forward Scattering Spectrometer Probe (FSSP-100) as described by de Reus et al. (2009).

Temperature and pressure were measured using commercial Rosemount sensors. Geolocation data were provided by the M-55 avionic system.

2.2 Estimation of available inorganic chlorine (Cl_y)

Ideally, Cl_y is determined by measuring all inorganic chlorine compounds, i.e. HCl, $ClONO_2$, Cl_2, ClO, OClO, HOCl, and Cl_2O_2. Unfortunately, during TROCCINOX and SCOUT-O_3, ClO was the only measured inorganic chlorine species. Thus Cl_y must be estimated differently. Here we use correlations with other tracers, based on the fact that the amount of Cl_y in a particular air mass increases with photochemical aging, and is higher for stratospheric air than for tropospheric air. A fairly accurate method for estimating stratospheric Cl_y is provided by Woodbridge et al. (1995), but it is based on measurements of the most abundant organic chlorine compounds, which are not available with adequate time resolution for the TROCCINOX and SCOUT-O_3 data sets.

Here, we estimate Cl_y from observed O_3 adopting the approach by Thornton et al. (2005). To derive a correlation representative for the region and time of our measurements, we used ACE-FTS satellite observations of O_3 and HCl in the latitude band 30° N–30° S made between November 2004 and February 2006. On average these data yield a robust linear correlation (Fig. 1a) in fair agreement with O_3–HCl relationships shown by Marcy et al. (2004). However, for $x(O_3)<100$ ppb variability is high with $x(HCl)=15\pm52$ ppt (mean and standard deviation) and the correlation tends to yield very low or even negative HCl mixing ratios. Therefore, x(HCl) was set constant to 27 ppt below 100 ppb O_3 (27 ppt is used to avoid a discontinuity at 100 ppb O_3 where the correlation yields 27 ppt). Using ACE-FTS measurements of a large number of inorganic and organic chlorine containing trace gases in the tropics averaged over the period of February 2004 to January 2005 (Nassar et al., 2006), a relationship between x(HCl) and $x(Cl_y)$ is established (Fig. 1b). Combining the two correlations yields $x(Cl_y)=8.3\times10^{-4}\,x(O_3)-0.033$ ppb for $x(O_3)>100$ ppb, and $x(Cl_y)=50$ ppt for $x(O_3)<100$ ppb. This compares well with mid latitude observations (Avallone et al., 1993) where $x(Cl_y)\approx0.001\,x(O_3)$, Obviously, the uncertainty in this relationship is rather large, particularly for air with $x(O_3)<100$ ppb (Fig. 1a), where both measurement uncertainties and real relative variability are greatest. However, as can also be seen in

Fig. 1a, $x(\mathrm{Cl_y})$ seems unlikely to exceed ≈150 ppt in tropospheric air, which, as will be shown below, is clearly too low to explain some of the observations of enhanced ClO by pure gas phase chemistry.

2.3 CLaMS modelling studies

The Chemical Lagrangian Model of the Stratosphere (CLaMS) (Konopka et al., 2004; McKenna et al., 2002a,b) is a hierarchy of models ranging from a box model to a 3-D Chemistry Transport Model (CTM) based on a Lagrangian transport concept in which the chemical evolution within individual air parcels is simulated along their trajectories, which are determined from ECMWF temperature data and wind fields. For this study the CLaMS modules are used in three different modes:

- CLaMS_ST: the stationary mode with no transport and no mixing, where the air parcels stay at constant location and the chemical composition is influenced only by the diurnal photochemical cycle. This mode is used to derive typical noontime ClO mixing ratios and chlorine activation.
- CLaMS_CTM: the 3-D CTM mode, in which advection and mixing are calculated. No detailed chemistry is calculated for simulations in the CTM mode. The focus of this simulation is on water vapour and the development of ice particles that form cirrus clouds. For this purpose, a novel CLaMS module to estimate Ice Water Content was employed. This module computes the conversion between gas phase water and ice water utilizing a temperature-dependent value for saturation over ice derived from freezing measurements in a simulation chamber (Gensch et al., 2008; Krämer et al., 2009; Möhler et al., 2005). Ice crystal number densities are parameterised as described in these references.
- CLaMS_BT: the back-trajectory mode, in which the full photochemistry is simulated along trajectories that end on selected points on the flight path. This mode is used for the case studies in this paper.

2.3.1 Estimation of typical noontime chlorine activation

We estimate typical noontime ClO mixing ratios – with and without heterogeneous activation – using the stationary box model simulation CLaMS_ST for the Darwin location of 13° S/131° E (for simplicity, we used this location for both campaigns in CLaMS_ST) and different O_3 mixing ratios from 1 to 1300 ppb (the O_3 mixing ratio was reset to its initial value after each diurnal cycle, as otherwise O_3 accumulated significantly over the course of the simulation). To approximately represent the typical conditions encountered during TROCCINOX and SCOUT-O_3, temperature, pressure, water vapour, and aerosol number densities were initialized from their relationship with ozone averaged over all relevant flights (Fig. 2a,b,d,e). NO_y, which plays a critical role for chlorine partitioning, was initialised using a midlatitude correlation from Michelson et al. (1998), which fits the NO_y and O_3 observations made during TROCCINOX and SCOUT-O_3 better than the tropical correlation from the same paper. This is probably caused by the fact that only a subset of flights during TROCCINOX and SCOUT-O_3 were performed in tropical air masses (Brunner et al., 2009; Huntrieser et al., 2007). Cl_y was initialised as a function of O_3 as described in Sect. 2.2, with HCl being the only inorganic chlorine species present at the start of the model run. The simulation was run until the midday chlorine partitioning had reached equilibrium for all conditions (up to 30 iterative 1-day-cycles).

For heterogeneous chemistry in these simulations, ice formation was disabled and only reactions on liquid aerosol were simulated. Although being unrealistic at low temperatures (ice formation is likely and often observed below ≈195 K), this simplification does not significantly affect heterogeneous activation rates, because reactions 1 to 3 on liquid aerosol have a strong negative temperature dependence and reaction probabilities γ below 195 K are comparable to those on ice surfaces for reactions 1 and 2 (Zhang et al., 1994; Hanson et al., 1994; Shi et al., 2001).

2.3.2 Simulation of cirrus occurrence

Gas phase water in CLaMS_CTM runs is initialised at the beginning of each simulation utilizing the specific humidity taken from ECMWF data. Boundaries are updated every CLaMS time step from ECMWF data as well. The formation of ice is parameterised either by using a conservative fixed value for saturation over ice of 100% (like used by ECMWF until September 2006) or a temperature dependent parameterisation for heterogeneous freezing (Gensch et al., 2008; Krämer et al., 2009; Möhler et al., 2005). This parameterisation results in saturation values between 120 and 140% in the 180 to 230 K temperature range. Water vapour with values above these saturation levels is removed from the gas phase and added to the ice water content (IWC). Water vapour and ice water content are transported and mixed like any other tracer or chemical species. Evaporation at 100% saturation and sedimentation of ice are considered, the latter by assuming a uniform particle density and size distribution, thus parameterising processes like re- and de-hydration.

2.3.3 Individual case study simulations

For the case studies presented in Sect. 4, simulations using the ClaMS_BT mode were performed along 10-day-back-trajectories from locations along the flight path where significant Cl-activation was observed. Observed temperatures were significantly colder than ECMWF temperatures. This offset was subtracted for each air parcel individually from the temperatures along the whole trajectory.

Consistent with the above estimate, $x(\mathrm{Cl_y})$ was initialised to be 50 ppt in the form of HCl. Total H_2O was initialised to be 10 parts per million (ppm). Also, $x(\mathrm{NO_y})$ was initialised from SIOUX observations (510 ppt). Ozone was initialised from FOZAN observations (≈50 ppb), but it was also varied for the sensitivity studies. $\mathrm{Br_y}$ (=$\mathrm{Br+BrO+HBr+BrONO_2+BrCl}$) was set to 1 ppt, but also sensitivity studies with more $\mathrm{Br_y}$ were performed. The remaining species were initialised from the Mainz 2-D model (Grooß et al., 1998).

Formation of and reactions on particles were treated by the CLaMS heterogeneous chemistry module that has been developed for reactions on stratospheric particles (McKenna et al., 2002a). To account for the different conditions in the tropical UTLS, the following adjustments were made:

- As in the stratosphere, the heterogeneous reactions were allowed to occur on ice and interstitial sulphate aerosol. Both particle types allow uptake of HNO_3. The formation threshold for ice particles was parameterised according to freezing experiments in the AIDA chamber for coated soot particles as condensation nuclei (Gensch et al., 2008; Krämer et al., 2009; Möhler et al., 2005). These experiments resulted in a temperature-dependent threshold of around 50% super-saturation for the observed temperatures.
- The interstitial sulphate aerosol was initialised with 0.1 ppb H_2SO_4 gas phase equivalent and an aerosol number density of 300 cm^{-1}. In contrast to the stratospheric code, a typical ice particle radius of 10 µm was defined and from that the particle number density was calculated using the steady state IWC (order of magnitude: 0.1 cm^{-3}).
- Dehydration of the air due to particle sedimentation is simulated by a simple parameterisation that is linked to the particle settling velocity (Grooß et al., 2002). The characteristic height parameter was adjusted to 3.5 km such that the observed total H_2O mixing ratio by FISH was reached towards the end of the simulation.

3 Results

Figure 3 shows that, during both campaigns, ClO generally increased together with ozone. This is consistent with the expected dependence of ClO on photochemical processing and available Cl_y: mixing ratios found in stratospheric air did not significantly exceed typical noontime ClO levels expected from the known gas phase chemistry, which were estimated by the CLaMS_ST simulations for gas-phase only and are represented by the black line in Fig. 3, with the grey shading representing uncertainties due to time of day and temperature. From the CLaMS_ST gas phase simulations, ClO is expected to remain below ≈2 ppt in air masses with a significant tropospheric fraction ($x(O_3)<300$ ppb) in agreement with a large number of ClO observations at or below the HALOX detection limit. However, during a number of flights, significantly enhanced mixing ratios of up to 40 ppt ClO were found, exceeding values expected for gas phase chemistry by about an order of magnitude. Only if heterogeneous chemistry is included in the CLaMS_ST simulations does the range of simulated noontime ClO mixing ratios – marked by the blue shaded area in Fig. 3 – correspond reasonably well to the high values that were sometimes observed, suggesting heterogeneous reactions causing substantial production of active chlorine in the TTL. This may be rationalised by the low temperatures prevalent in the TTL leading to high heterogeneous reaction rates. Indeed, the highest degree of chlorine activation – given by the $x(ClO)/x(Cl_y)$ ratio following Thornton et al. (2003) – was found in air masses with low ozone but also very low temperatures (Fig. 4), where heterogeneous reactions are most likely to play a relevant role. We further investigated the correspondence of Cl activation and cirrus/ice particle presence using simultaneous measurements of aerosol depolarization (MAS), temperature and ice water content (FISH), plus simulations of the latter two parameters on back trajectories in the CLaMS_CTM mode. Figure 5 shows a correlation of the relative chlorine activation with ozone. It is evident that most events of enhanced ClO are linked to either temperatures <195 K and/or the occurrence of cirrus clouds during or preceding the flight. This is a strong indication that elevated ClO mixing ratios observed during TROCCINOX and SCOUT-O_3 were caused by heterogeneous chlorine activation proceeding on cirrus ice particles and/or background aerosol at low temperatures. Transport of substantial amounts of ClO into the TTL from the stratosphere can be ruled out because this would also lead to an increase in $x(O_3)$. Substantial mixing ratios of several 100 ppt inorganic chlorine have been observed in the marine boundary layer (Pszenny et al., 1993), but rapid and quantitative transport to the TTL seems unwarranted due to loss by wet deposition. Moreover, neither observations (e.g. tracers, water vapour, etc.) nor trajectory calculations support direct transport of boundary layer air to the TTL for the probed air masses with elevated ClO mixing ratios during TROCCINOX and SCOUT-O_3.

Observed ClO mixing ratios were generally higher during SCOUT-O_3 than during TROCCINOX. One explanation may be the higher altitude of the tropopause and the observed cirrus clouds and therefore possibly a higher abundance of Cl_y that can be activated during the SCOUT-O_3 campaign in Darwin. The tropopause was also significantly colder during SCOUT-O_3 than during TROCCINOX (Fig. 2a) resulting in faster heterogeneous processing on background aerosol and more extensive and prolonged cirrus formation during SCOUT-O_3. This conclusion is supported by the CLaMS simulation.

4 Case studies – investigation of the Cl activation mechanism

Figure 6 shows enhanced ClO clearly associated with cirrus clouds during two SCOUT-O_3 flights on 19 and 30 November 2005. Elevated ClO always concurs with low temperature and the presence of ice water as indicated by the elevated FISH total water mixing ratios and the presence of large particles – most likely ice – detected by the FSSP instrument. As shown in the lower panels of Fig. 6, the distribution of water vapour around the flight track – estimated using CLaMS_CTM – suggests highest ClO levels near the top of cirrus clouds. Interestingly, the observations on 30 November were made in darkness (SZA>100°), where significant amounts of ClO are unexpected.

Both flights were investigated in detail using the CLaMS_BT chemistry simulation along back trajectories described in Sect. 2.3. Figure 7 shows the simulation results for the flight on 19 November 2005 along one chosen back-trajectory for a time window where high chlorine activation was observed by HALOX. Using the observed mixing ratios of ozone, NO_y, and H_2O, the simulation did not reproduce the observed ClO mixing ratios. However, the simulation indeed shows the observed almost complete chlorine activation in sensitivity studies run with higher Br_y and/or O_3 mixing ratios (Fig. 7). For the runs with 200 ppb O_3, CLaMS_BT predicts ClO to be present in significant amounts during night-time, together with the main night-time reservoir species OClO. This is also the case for the 30 November simulation shown in Fig. 8.

The mechanism of chlorine activation implemented in CLaMS (both CLaMS_ST and CLaMS_BT) is illustrated in Fig. 9. In the presence of ice surfaces and light, chlorine activation is possible by the following reaction chains

$$
\begin{array}{llll}
 & \mathrm{ClO + NO_2} & \rightarrow \mathrm{ClONO_2} & \text{(R5)} \\
 & \mathrm{HCl + ClONO_2} & \rightarrow \mathrm{Cl_2 + HNO_3} & \text{(R1, heterogeneous)} \\
 & \mathrm{Cl_2} + h\nu & \rightarrow \mathrm{2Cl} & \text{(R6)} \\
2\times & \mathrm{Cl + O_3} & \rightarrow \mathrm{ClO + O_2} & \text{(R7)} \\
\hline
\text{Net:} & \mathrm{HCl + NO_2 + 2O_3} & \rightarrow \mathrm{ClO + HNO_3 + 2O_2} & \text{(chain 1),}
\end{array}
$$

$$
\begin{array}{llll}
 & \mathrm{ClO + HO_2} & \rightarrow \mathrm{HOCl + O_2} & \text{(R8)} \\
 & \mathrm{HCl + HOCl} & \rightarrow \mathrm{Cl_2 + H_2O} & \text{(R2, het.)} \\
 & \mathrm{Cl_2} + h\nu & \rightarrow \mathrm{2Cl} & \text{(R6)} \\
2\times & \mathrm{Cl + O_3} & \rightarrow \mathrm{ClO + O_2} & \text{(R7)} \\
\hline
\text{Net:} & \mathrm{HCl + HO_2 + 2O_3} & \rightarrow \mathrm{ClO + H_2O + 3O_2} & \text{(chain 2)}
\end{array}
$$

and

$$
\begin{array}{llll}
 & \mathrm{ClO + NO_2} & \rightarrow \mathrm{ClONO_2} & \text{(R5)} \\
 & \mathrm{H_2O + ClONO_2} & \rightarrow \mathrm{HOCl + HNO_3} & \text{(R3, het.)} \\
 & \mathrm{HCl + HOCl} & \rightarrow \mathrm{Cl_2 + H_2O} & \text{(R2, het.)} \\
 & \mathrm{Cl_2} + h\nu & \rightarrow \mathrm{2Cl} & \text{(R6)} \\
2\times & \mathrm{Cl + O_3} & \rightarrow \mathrm{ClO + O_2} & \text{(R7)} \\
\hline
\text{Net:} & \mathrm{HCl + NO_2 + 2O_3} & \rightarrow \mathrm{ClO + HNO_3 + 2O_2} & \text{(chain 3)}
\end{array}
$$

Although all these chains start with a deactivation reaction, two chlorine reservoir molecules are activated by the following heterogeneous reaction resulting in a net chlorine activation (Müller et al., 1994). At the same time as they activate chlorine, chains 1 and 3 remove NO_x from the gas phase into the particle phase as HNO_3.

These reactions are counteracted by the chlorine deactivation reaction

$$Cl + CH_4 \rightarrow HCl + CH_3 . \tag{9}$$

The net chlorine activation through chains 1–3 can only take place if the overall activation rate is faster than the chlorine deactivation via R9. The simulations show that once low NO_x levels are reached (by removal through chains 1 and 3), chlorine partitioning suddenly switches from low to almost complete activation. The reason for this behaviour will be explained below. The sensitivity studies show that the occurrence of this threshold is especially sensitive to Br_y and O_3 levels.

During daytime, when ClO is present, reaction R5 is slow due to most NO_x being present in the form of NO. To understand the dependencies of chlorine activation on $x(Br_y)$ and $x(O_3)$, the ratios $x(Cl)/x(ClO)$ and $x(NO_2)/x(NO)$ are critical. Under tropical daytime conditions in the TTL, $x(Cl)/x(ClO)$ is determined by reactions R7 and

$$ClO + NO \rightarrow Cl + NO_2 . \tag{10}$$

and can be approximated by

$$\frac{x(Cl)}{x(ClO)} = \frac{c(Cl)}{c(ClO)} = \frac{k_{10} c(NO)}{k_7 c(O_3)} \tag{1}$$

assuming photochemical steady state.

Similarly, the $x(NO_2)/x(NO)$ ratio is determined by R10,

$$BrO + NO \rightarrow Br + NO_2 , \tag{R11}$$

$$O_3 + NO \rightarrow O_2 + NO_2 , \text{ and} \tag{R12}$$

$$NO_2 + h\nu \rightarrow NO + O \tag{R13}$$

giving

$$\frac{x(\mathrm{NO_2})}{x(\mathrm{NO})} = \frac{c(\mathrm{NO_2})}{c(\mathrm{NO})} = \frac{k_{10}c(\mathrm{ClO}) + k_{11}c(\mathrm{BrO}) + k_{12}c(\mathrm{O_3})}{J_{13}} \tag{2}$$

The simulations show that chain 1 is most important in the case of low chlorine activation. The chlorine activation rate $R_{\mathrm{Act\_1}}$ through chain 1 is given by

$$R_{\mathrm{Act\_1}} = k_5 c(\mathrm{ClO}) c(\mathrm{NO_2}) \tag{3}$$

which, using Eq. (2), becomes

$$R_{\mathrm{Act\_1}} = k_5 c(\mathrm{ClO}) c(\mathrm{NO}) \frac{k_{10}c(\mathrm{ClO}) + k_{11}c(\mathrm{BrO}) + k_{12}c(\mathrm{O_3})}{J_{13}}. \tag{4}$$

The deactivation rate $R_{\mathrm{Deact\_9}}$ through reaction R1 is given by

$$R_{\mathrm{Deact\_9}} = k_9 c(\mathrm{Cl}) c(\mathrm{CH_4}) \tag{5}$$

which, using Eq. (1), becomes

$$R_{\mathrm{Deact\_9}} = \frac{k_9 k_{10} c(\mathrm{NO}) c(\mathrm{ClO}) c(\mathrm{CH_4})}{k_7 c(\mathrm{O_3})} \tag{6}$$

A sufficient condition for chlorine activation in the presence of ice surfaces is given if the chlorine activation rate exceeds the deactivation rate:

$$\frac{R_{\mathrm{Act\_1}}}{R_{\mathrm{Deact\_9}}} = \frac{k_5 k_7 c(\mathrm{O_3})}{k_9 k_{10} J_{13}} \frac{k_{10}c(\mathrm{ClO}) + k_{11}c(\mathrm{BrO}) + k_{12}c(\mathrm{O_3})}{c(\mathrm{CH_4})} > 1. \tag{7}$$

The simulations show that $\mathrm{NO_x}$ is converted to $\mathrm{HNO_3}$ by chains 1 and 3 (with chain 1 dominating). If very low $\mathrm{NO_x}$ mixing ratios are reached, chains 1 and 3 do not work anymore and further chlorine activation can only occur via chain 2.

The condition formulated above (Eq. 7) is independent of $\mathrm{NO_x}$. Simulations demonstrate that in the case that chlorine is already activated, the chlorine activation chains keep working, even if NO_x is added. However, in this case, NO_x is converted to HNO_3 at a rate of about 150 ppt/day through chain 1.

The dependence of R_{Act_1}/R_{Deact_9} (Eq. 7) on ClO itself is the main reason for the threshold-like behaviour of chlorine activation. If some chlorine is activated and is in the form of ClO, the effective activation rate increases. This causes a hysteresis-like behaviour in chlorine activation: under otherwise identical conditions, air masses with activated chlorine may stay activated whereas air masses without chlorine activation may not be activated at all. In the case of full activation an almost complete removal of NO_x is simulated.

Although chlorine activation is not simulated using the observed mixing ratios of O_3, BrO and NO_x, it has been shown that the point at which the system switches to chlorine activation sensitively depends on a number of factors. Possible uncertainties are present in the simulation e.g. the reaction rates or possible omitted chemical reactions, and temperatures along the back-trajectory. A Gaussian error propagation of R_{Act_1}/R_{Deact_9} in Eq. (7) with respect to uncertainties of the individual rate constants (Sander et al., 2006) at 200 K yields an uncertainty of about a factor 3. Further, there are indications that the formation of HOCl from $ClO+HO_2$ may be faster than recommended (Kovalenko et al., 2007; Stimpfle et al., 1979; von Clarmann et al., 2009). If these indications were true the Cl activation would be even faster. To illustrate the complex sensitivity of chlorine activation on various mixing ratios and rate constants, we plotted in Fig. 10 the ClO mixing ratio on the final day of the trajectory that ends on the observed point with high chlorine activation for different initial ozone mixing ratios. The red symbols show results for the 1 ppt Br_y and the standard set of chemical reactions. A full Cl-activation is found for ozone mixing ratios above a threshold of about 185 ppb. The precise location of this threshold depends on model parameters.

If for the reaction ($ClO+HO_2$) a faster rate coefficient is assumed as suggested by (Kovalenko et al., 2007; Stimpfle et al., 1979; von Clarmann et al., 2009), the threshold for full chlorine activation is found at slightly lower ozone mixing ratios (blue symbols in Fig. 10). In addition, there are assumptions in this simulation that also introduce uncertainty in the heterogeneous reaction rates. A sensitivity study was performed using an increase of all heterogeneous reaction rates by a factor of 5 (green symbols). This would correspond to using the lower climatological limit of ice particle radius of about 2 µm (Gensch et al., 2008; Krämer et al., 2009; Möhler et al., 2005). The uncertainty of gas-phase reaction rate coefficients at temperatures below 190 K is also significant. The orange symbols show simulations in which the reaction rate coefficient of the reaction O_3+NO is changed to the upper error limit of the recommended value. The brown symbols correspond to the upper error limit of the recommended value for the reaction (ClO+NO_2). The position of the threshold also depends on the amount of available Br_y. The remaining symbols (light blue, pink, light grey, dark grey) correspond to higher assumptions for Br_y mixing ratios (2, 3, 4, and 5 ppt, respectively). A combination of all changes with the assumption of 5 ppt Br_y would result in full chlorine activation at 50 ppb O_3.

The simulation of NO_x from the box model simulation along the back-trajectory did result in much lower values than observed. The reason for the large measured NO_x values is most probably in-situ NO_x production by lightning in Hector and other single cell continental thunderstorms in the measurement area (Huntrieser et al., 2009). According to Eq. (7), the threshold value for chlorine activation is independent of NO_x. Thus, in-mixing of NO_x-rich air or in-situ NO_x production for air masses with chlorine activation would leave the air masses activated. This assumption was verified by a sensitivity simulation, in which 300 ppt of the prevailing HNO_3 was artificially reformed into NO_x (not shown). Indeed, the change of NO_x did leave the model in the chlorine-activated state. However, within about one day, the major fraction of the additional NO_x was reformed back to HNO_3 through reaction chains 1 and 3.

5 Conclusions

Observations of ClO in the tropics between 11 and 20 km altitude were made during two aircraft campaigns in 2005. In general, higher ClO mixing ratios were found in air masses of stratospheric origin, but incidences of enhanced ClO of up to 40 ppt in tropospherically dominated air masses were observed during and after cirrus events and/or following periods of relatively low temperatures. Thus there is strong evidence for heterogeneous chlorine activation proceeding in the tropical UTLS on both ice particles and background aerosol at low temperature, although our results do not provide sufficient evidence to assess the relative importance of the two. As demonstrated by CLaMS_ST and CLaMS_CTM simulations, the amount of active chlorine that can be produced by heterogeneous activation, and consequently ClO mixing ratios in the tropical UTLS, depend most strongly on the availability of Cl_y and on the persistence of temperatures below ≈195 K and/or the life-time of the cirrus clouds. With the CLaMS_BT simulations for the case studies we could demonstrate that an almost complete chlorine activation near the tropopause is possible but depends on many factors. Because of competing activation and deactivation chains, different Cl activation may be found in similar air masses. With the known chemical mechanisms and rate constants, the conditions at which the CLaMS model predicts complete activation is most sensitive to O_3 and Br_y concentrations, with uncertainties in individual reaction rate constants leading to a significant uncertainty in the threshold condition for the domination of the chlorine activation chain.

Clearly, the model parameters used in the CLaMS model runs where almost complete activation was simulated do not correspond closely to observations, in particular with respect to observed O_3 and NO_x levels, suggesting that the understanding and, consequently, model implementation of the relevant chemical processes in the TTL is yet incomplete. Part of the discrepancies may be explained by uncertainties in rate constants and Br_y levels, and/or mixing processes within less than one day prior to the observations.

Acknowledgements. The authors thank MDB for their support of the Geophysica operations during the field campaigns and for the supply of avionic data. For organisation of and support during field campaigns, we are also grateful to the airport teams in Aracatuba and Darwin, and to the TROCCINOX and SCOUT-O_3 coordinating and mission planning teams. We further thank ECMWF for meteorological analyses, and the ACE-FTS Team for permission to use the satellite data. The TROCCINOX project was funded by the EU under the grant number EVK2-2001-00087. SCOUT-O_3 was funded by the EU under the grant number 505390-GOCE-CT-2004.

References

Avallone, L. M., Toohey, D. W., Brune, W. H., Salawitch, R. J., Dessler, A. E., and Anderson, J. G.: Balloon-borne in-situ measurements of ClO and ozone – implications for heterogeneous chemistry and midlatitude ozone loss, Geophys. Res. Lett., 20, 1795–1798, 1993.

Borrmann, S., Solomon, S., Dye, J. E., and Luo, B. P.: The potential of cirrus clouds for heterogeneous chlorine activation, Geophys. Res. Lett., 23, 2133–2136, 1996.

Borrmann, S., Solomon, S., Avallone, L., Toohey, D., and Baumgardner, D.: On the occurrence of ClO in cirrus clouds and volcanic aerosol in the tropopause region, Geophys. Res. Lett., 24, 2011–2014, 1997.

Bregman, B., Wang, P. H., and Lelieveld, J.: Chemical ozone loss in the tropopause region on subvisible ice clouds, calculated with a chemistry-transport model, J. Geophys. Res., 107, 4032, doi:10.1029/2001JD000761, 2002.

Brune, W. H., Anderson, J. G., and Chan, K. R.: Insitu observations of ClO in the antarctic – ER-2 aircraft results from 54-degrees-S to 72-degrees-S latitude, J. Geophys. Res., 94, 16649–16663, 1989.

Brunner, D., Siegmund, P., May, P. T., Chappel, L., Schiller, C., Müller, R., Peter, T., Fueglistaler, S., MacKenzie, A. R., Fix, A., Schlager, H., Allen, G., Fjaeraa, A. M., Streibel, M., and Harris, N. R. P.: The SCOUT-O_3 Darwin Aircraft Campaign: rationale and meteorology, Atmos. Chem. Phys., 9, 93–117, doi:10.5194/acp-9-93-2009, 2009.

Buontempo, C., Cairo, F., Di Donfrancesco, G., Morbidini, R., Viterbini, M., and Adriani, A.: Optical measurements of atmospheric particles from airborne platforms: in situ and remote sensing instruments for balloons and aircrafts, Ann. Geophys., 49, 57–65, 2006, http://www.ann-geophys.net/49/57/2006/.

de Reus, M., Borrmann, S., Bansemer, A., Heymsfield, A. J., Weigel, R., Schiller, C., Mitev, V., Frey, W., Kunkel, D., Kürten, A., Curtius, J., Sitnikov, N. M., Ulanovsky, A., and Ravegnani, F.: Evidence for ice particles in the tropical stratosphere from in-situ measurements, Atmos. Chem. Phys., 9, 6775–6792, doi:10.5194/acp-9-6775-2009, 2009.

Dorf, M., Butler, J. H., Butz, A., Camy-Peyret, C., Chipperfield, M. P., Kritten, L., Montzka, S. A., Simmes, B., Weidner, F., and Pfeilsticker, K.: Long-term observations of stratospheric bromine reveal slow down in growth, Geophys. Res. Lett., 33, L24803, doi:10.1029/2005GL025466, 2006.

Fusco, A. C. and Salby, M. L.: Interannual variations of total ozone and their relationship to variations of planetary wave activity, J. Climate, 12, 1619–1629, 1999.

Gensch, I. V., Bunz, H., Baumgardner, D. G., Christensen, L. E., Fahey, D. W., Herman, R. L., Popp, P. J., Smith, J. B., Troy, R. F., Webster, C. R., Weinstock, E. M., Wilson, J. C., Peter, T., and Krämer, M.: Supersaturations, microphysics and nitric acid partitioning in a cold cirrus cloud observed during CR-AVE 2006: an observation-modelling intercomparison study, Environ. Res. Lett., 3, 035003, 2008.

Grooß, J. U., Günther, G., Konopka, P., Müller, R., McKenna, D. S., Stroh, F., Vogel, B., Engel, A., Muller, M., Hoppel, K., Bevilacqua, R., Richard, E., Webster, C. R., Elkins, J. W., Hurst, D. F., Romashkin, P. A., and Baumgardner, D. G.: Simulation of ozone depletion in spring 2000 with the Chemical Lagrangian Model of the Stratosphere (CLaMS), J. Geophys. Res., 107, 8295, doi:10.1029/2001JD000933, 2002.

Grooß, J. U., Brühl, C., and Peter, T.: Impact of aircraft emissions on tropospheric and stratospheric ozone, Part 1: Chemistry and 2-D model results, Atmos. Environ., 32, 3173–3184, 1998.

Hanson, D. R., Ravishankara, A. R., and Solomon, S.: Heterogeneous reactions in sulfuric-acid aerosols – a framework for model-calculations, J. Geophys. Res., 99, 3615–3629, 1994.

Hood, L. L. and Soukharev, B. E.: Interannual variations of total ozone at northern midlatitudes correlated with stratospheric EP flux and potential vorticity, J. Atmos. Sci., 62, 3724–3740, 2005.

Huntrieser, H., Schlager, H., Roiger, A., Lichtenstern, M., Schumann, U., Kurz, C., Brunner, D., Schwierz, C., Richter, A., and Stohl, A.: Lightning-produced NO_x over Brazil during TROCCINOX: airborne measurements in tropical and subtropical thunderstorms and the importance of mesoscale convective systems, Atmos. Chem. Phys., 7, 2987–3013, doi:10.5194/acp-7-2987-2007, 2007.

Huntrieser, H., Schlager, H., Lichtenstern, M., Roiger, A., Stock, P., Minikin, A., Höller, H., Schmidt, K., Betz, H.-D., Allen, G., Viciani, S., Ulanovsky, A., Ravegnani, F., and Brunner, D.: NO_x production by lightning in Hector: first airborne measurements during SCOUT-O_3/ACTIVE, Atmos. Chem. Phys., 9, 8377–8412, doi:10.5194/acp-9-8377-2009, 2009.

Keim, E. R., Fahey, D. W., DelNegro, L. A., Woodbridge, E. L., Gao, R. S., Wennberg, P. O., Cohen, R. C., Stimpfle, R. M., Kelly, K. K., Hintsa, E. J., Wilson, J. C., Jonsson, H. H., Dye, J. E., Baumgardner, D., Kawa, S. R., Salawitch, R. J., Proffitt, M. H., Loewenstein, M., Podolske, J. R., and Chan, K. R.: Observations of large reductions in the NO/NO_y ratio near the mid-latitude tropopause and the role of heterogeneous chemistry, Geophys. Res. Lett., 23, 3223–3226, 1996.

Konopka, P., Steinhorst, H. M., Grooß, J. U., Günther, G., Müller, R., Elkins, J. W., Jost, H. J., Richard, E., Schmidt, U., Toon, G., and McKenna, D. S.: Mixing and ozone loss in the 1999–2000 Arctic vortex: Simulations with the three-dimensional Chemical Lagrangian Model of the Stratosphere (CLaMS),J. Geophys. Res., 109, D02315, doi:10.1029/2003JD003792, 2004.

Konopka, P., Günther, G., Müller, R., dos Santos, F. H. S., Schiller, C., Ravegnani, F., Ulanovsky, A., Schlager, H., Volk, C. M., Viciani, S., Pan, L. L., McKenna, D.-S., and Riese, M.: Contribution of mixing to upward transport across the tropical tropopause layer (TTL), Atmos. Chem. Phys., 7, 3285–3308, doi:10.5194/acp-7-3285-2007, 2007.

Kovalenko, L. J., Jucks, K. W., Salawitch, R. J., Toon, G. C., Blavier, J. F., Johnson, D. G., Kleinbohl, A., Livesey, N. J., Margitan, J. J., Pickett, H. M., Santee, M. L., Sen, B., Stachnik, R. A., and Waters, J. W.: Observed and modeled HOCl profiles in the midlatitude stratosphere: implication for ozone loss, Geophys. Res. Lett., 34, L19801, doi:10.1029/2007GL031100, 2007.

Krämer, M., Schiller, C., Afchine, A., Bauer, R., Gensch, I., Mangold, A., Schlicht, S., Spelten, N., Sitnikov, N., Borrmann, S., de Reus, M., and Spichtinger, P.: Ice supersaturations and cirrus cloud crystal numbers, Atmos. Chem. Phys., 9, 3505–3522, doi:10.5194/acp-9-3505-2009, 2009.

Logan, J. A.: An analysis of ozonesonde data for the lower stratosphere: Recommendations for testing models, J. Geophys. Res., 104, 16151–16170, 1999.

Marcy, T. P., Fahey, D. W., Gao, R. S., Popp, P. J., Richard, E. C., Thompson, T. L., Rosenlof, K. H., Ray, E. A., Salawitch, R. J., Atherton, C. S., Bergmann, D. J., Ridley, B. A., Weinheimer, A. J., Loewenstein, M., Weinstock, E. M., and Mahoney, M. J.: Quantifying stratospheric ozone in the upper troposphere with in situ measurements of HCl, Science, 304, 261–265, 2004.

McKenna, D. S., Grooß, J. U., Günther, G., Konopka, P., Müller, R., Carver, G., and Sasano, Y.: A new Chemical Lagrangian Model of the Stratosphere (CLaMS) – 2. Formulation of chemistry scheme and initialization, J. Geophys. Res., 107, 4256, doi:10.1029/2000JD000113, 2002a.

McKenna, D. S., Konopka, P., Grooß, J. U., Günther, G., Müller, R., Spang, R., Offermann, D., and Orsolini, Y.: A new Chemical Lagrangian Model of the Stratosphere (CLaMS) – 1. Formulation of advection and mixing, J. Geophys. Res., 107, 4309, doi:10.1029/2000JD000114, 2002b.

Michelson, H. A., Manney, G. L., Gunson, M. R., and Zander, R.: Correlations of stratospheric abundances of NO_y, O_3, N_2O, and CH_4 derived from ATMOS measurements, J. Geophys. Res., 103, 28347–28359, 1998.

Möhler, O., Buttner, S., Linke, C., Schnaiter, M., Saathoff, H., Stetzer, O., Wagner, R., Krämer, M., Mangold, A., Ebert, V., and Schurath, U.: Effect of sulfuric acid coating on heterogeneous ice nucleation by soot aerosol particles, J. Geophys. Res., 110, D11210, doi:10.1029/2004JD005169, 2005.

Müller, R., Peter, T., Crutzen, P. J., Oelhaf, H., Adrian, G. P., Vonclarmann, T., Wegner, A., Schmidt, U., and Lary, D.: Chlorine chemistry and the potential for ozone depletion in the Arctic stratosphere in the winter of 1991/92, Geophys. Res. Lett., 21, 1427–1430, 1994.

Nassar, R., Bernath, P. F., Boone, C. D., Clerbaux, C., Coheur, P. F., Dufour, G., Froidevaux, L., Mahieu, E., McConnell, J. C., McLeod, S. D., Murtagh, D. P., Rinsland, C. P., Semeniuk, K., Skelton, R., Walker, K. A., and Zander, R.: A global inventory of stratospheric chlorine in 2004, J. Geophys. Res., 111, D22312, doi:10.1029/2006JD007395, 2006.

Pszenny, A. A. P., Keene, W. C., Jacob, D. J., Fan, S., Maben, J. R., Zetwo, M. P., Springer-young, M., and Galloway, J. N.: Evidence of inorganic chlorine gases other than hydrogen-chloride in marine surface air, Geophys. Res. Lett., 20, 699–702, 1993.

Ramaswamy, V., Chanin, M. L., Angell, J., Barnett, J., Gaffen, D., Gelman, M., Keckhut, P., Koshelkov, Y., Labitzke, K., Lin, J. J. R., O'Neill, A., Nash, J., Randel, W., Rood, R., Shine, K., Shiotani, M., and Swinbank, R.: Stratospheric temperature trends: Observations and model simulations, Rev. Geophys., 39, 71–122, 2001.

Salawitch, R. J., Weisenstein, D. K., Kovalenko, L. J., Sioris, C. E., Wennberg, P. O., Chance, K., Ko, M. K. W., and McLinden, C. A.: Sensitivity of ozone to bromine in the lower stratosphere, Geophys. Res. Lett., 32, L05811, doi:10.1029/2004GL021504, 2005.

Salby, M. L. and Callaghan, P. F.: Systematic changes of Northern Hemisphere ozone and their relationship to random interannual changes, J. Quant. Spectrosc. Ra., 17, 4512–4521, 2004.

Sander, S. P., Finlayson-Pitts, B. J., Friedl, R. R., Golden, D. M., Huie, R. E., Keller-Rudek, H., Kolb, C. E., Kurylo, M. J., Molina, M. J., Moortgat, G. K., Orkin, V. L., Ravishankara, A. R., and Wine, P. H.: Chemical Kinetics and Photochemical Data for Use in Atmospheric Studies, Jet Propulsion Laboratory, Pasadena06-2, 2006.

Schiller, C., Krämer, M., Afchine, A., Spelten, N., and Sitnikov, N.: Ice water content of Arctic, midlatitude, and tropical cirrus, J. Geophys. Res., 113, D24208, doi:10.1029/2008JD010342, 2008.

Schiller, C., Grooß, J.-U., Konopka, P., Plöger, F., Silva dos Santos, F. H., and Spelten, N.: Hydration and dehydration at the tropical tropopause, Atmos. Chem. Phys., 9, 9647–9660, doi:10.5194/acp-9-9647-2009, 2009

Schmitt, J.: Construction and testing of an in-situ NO/NO_y measuring system aboard the high-altitude research aircaft M55-Geophysica, PhD thesis, University of Munich, 2003.

Schwab, J. J. and Anderson, J. G.: Oscillator strength of Cl(I) in the vacuum ultraviolet: the 2D-2P transitions., J. Quant. Spectrosc. Ra., 27, 445–457, 1982.

Shi, Q., Jayne, J. T., Kolb, C. E., Worsnop, D. R., and Davidovits, P.: Kinetic model for reaction of $ClONO_2$ with H_2O and HCl and HOCl with HCl in sulfuric acid solutions, J. Geophys. Res., 106, 24259–24274, 2001.

Sitnikov, N. M., Yushkov, V. A., Afchine, A. A., Korshunov, L. I., Astakhov, V. I., Ulanovskii, A. E., Kraemer, M., Mangold, A., Schiller, C., and Ravegnani, F.: The FLASH instrument for water vapor measurements on board the high-altitude airplane, Instrum. Exp. Tech., 50, 113–121, 2007.

Solomon, S., Garcia, R. R., Rowland, F. S., and Wuebbles, D. J.: On the depletion of Antarctic ozone, Nature, 321, 755–758, 1986.

Solomon, S., Borrmann, S., Garcia, R. R., Portmann, R., Thomason, L., Poole, L. R., Winker, D., and McCormick, M. P.: Heterogeneous chlorine chemistry in the tropopause region, J. Geophys. Res., 102, 21411–21429, 1997.

Stimpfle, R. M., Perry, R. A., and Howard, C. J.: Temperature-dependence of the reaction of ClO and HO_2 radicals, J. Chem. Phys., 71, 5183–5190, 1979.

Stroh, F., Grooß, J.-U., von Hobe, M., Hrechanyy, S., and Winkler, U.: Enhanced ClO Mixing ratios in the arctic polar winter UTLS region, XX Quadrennial Ozone Symposium, Kos, Greece, 724, 2004.

Thornton, B. F., Toohey, D. W., Avallone, L. M., Harder, H., Martinez, M., Simpas, J. B., Brune, W. H., and Avery, M. A.: In situ observations of ClO near the winter polar tropopause, J. Geophys. Res., 108, 8333, doi:10.1029/2002JD002839, 2003.

Thornton, B. F., Toohey, D. W., Avallone, L. M., Hallar, A. G., Harder, H., Martinez, M., Simpas, J. B., Brune, W. H., Koike, M., Kondo, Y., Takegawa, N., Anderson, B. E., and Avery, M. A.: Variability of active chlorine in the lowermost Arctic stratosphere, J. Geophys. Res., 110, D22304, doi:10.1029/2004JD005580, 2005.

Ulanovsky, A. E., Yushkov, V. A., Sitnikov, N. M., and Ravengnani, F.: The FOZAN-II fast-response chemiluminescent airborne ozone analyzer, Instrum. Exp. Tech., 44, 249–256, 2001.

Voigt, C., Schlager, H., Luo, B. P., Dörnbrack, A., Roiger, A., Stock, P., Curtius, J., Vössing, H., Borrmann, S., Davies, S., Konopka, P., Schiller, C., Shur, G., and Peter, T.: Nitric Acid Trihydrate (NAT) formation at low NAT supersaturation in Polar Stratospheric Clouds (PSCs), Atmos. Chem. Phys., 5, 1371–1380, doi:10.5194/acp-5-1371-2005, 2005.

Voigt, C., Kärcher, B., Schlager, H., Schiller, C., Krämer, M., de Reus, M., Vössing, H., Borrmann, S., and Mitev, V.: In-situ observations and modeling of small nitric acid-containing ice crystals, Atmos. Chem. Phys., 7, 3373–3383, doi:10.5194/acp-7-3373-2007, 2007.

von Clarmann, T., Glatthor, N., Ruhnke, R., Stiller, G. P., Kirner, O., Reddmann, T., Höpfner, M., Kellmann, S., Kouker, W., Linden, A., and Funke, B.: HOCl chemistry in the Antarctic Stratospheric Vortex 2002, as observed with the Michelson Interferometer for Passive Atmospheric Sounding (MIPAS), Atmos. Chem. Phys., 9, 1817–1829, doi:10.5194/acp-9-1817-2009, 2009.

von Hobe, M., Grooß, J.-U., Müller, R., Hrechanyy, S., Winkler, U., and Stroh, F.: A re-evaluation of the ClO/Cl_2O_2 equilibrium constant based on stratospheric in-situ observations, Atmos. Chem. Phys., 5, 693–702, doi:10.5194/acp-5-693-2005, 2005.

Wang, P. H., Minnis, P., McCormick, M. P., Kent, G. S., and Skeens, K. M.: A 6-year climatology of cloud occurence frequency from Stratospheric Aerosol and Gas Experiment II observations (1985–1990), J. Geophys. Res., 101, 29407–29429, 1996.

Weigel, R., Hermann, M., Curtius, J., Voigt, C., Walter, S., Böttger, T., Lepukhov, B., Belyaev, G., and Borrmann, S.: Experimental characterization of the COndensation PArticle counting System for high altitude aircraft-borne application, Atmos. Meas. Tech., 2, 243–258, doi:10.5194/amt-2-243-2009, 2009.

WMO: Scientific assessment of ozone depletion, World Meteorological Organization, Global

Title Page
Abstract | Introduction
Conclusions | References
Tables | Figures
◀| | |▶
◀ | ▶
Back | Close
Full Screen / Esc
Printer-friendly Version
Interactive Discussion

ozone research and monitoring project, Geneva, Switzerland 50, 2006.

Woodbridge, E. L., Elkins, J. W., Fahey, D. W., Heidt, L. E., Solomon, S., Baring, T. J., Gilpin, T. M., Pollock, W. H., Schauffler, S. M., Atlas, E. L., Loewenstein, M., Podolske, J. R., Webster, C. R., May, R. D., Gilligan, J. M., Montzka, S. A., Boering, K. A., and Salawitch, R. J.: Estimates of total organic and inorganic chlorine in the lower stratosphere from in-situ and flask measurements during AASE-II, J. Geophys. Res., 100, 3057–3064, 1995.

Yushkov, V., Oulanovsky, A., Lechenuk, N., Roudakov, I., Arshinov, K., Tikhonov, F., Stefanutti, L., Ravegnani, F., Bonafe, U., and Georgiadis, T.: A chemiluminescent analyzer for stratospheric measurements of the ozone concentration (FOZAN), J. Atmos. Ocean. Technol., 16, 1345–1350, 1999.

Zhang, R. Y., Leu, M. T., and Keyser, L. F.: Heterogeneous reactions of $ClONO_2$, HCl, and HOCl on liquid sulfuric-acid surfaces, J. Phys. Chem., 98, 13563–13574, 1994.

Zöger, M., Afchine, A., Eicke, N., Gerhards, M. T., Klein, E., McKenna, D. S., Morschel, U., Schmidt, U., Tan, V., Tuitjer, F., Woyke, T., and Schiller, C.: Fast in situ stratospheric hygrometers: A new family of balloon-borne and airborne Lyman alpha photofragment fluorescence hygrometers, J. Geophys. Res., 104, 1807–1816, 1999.

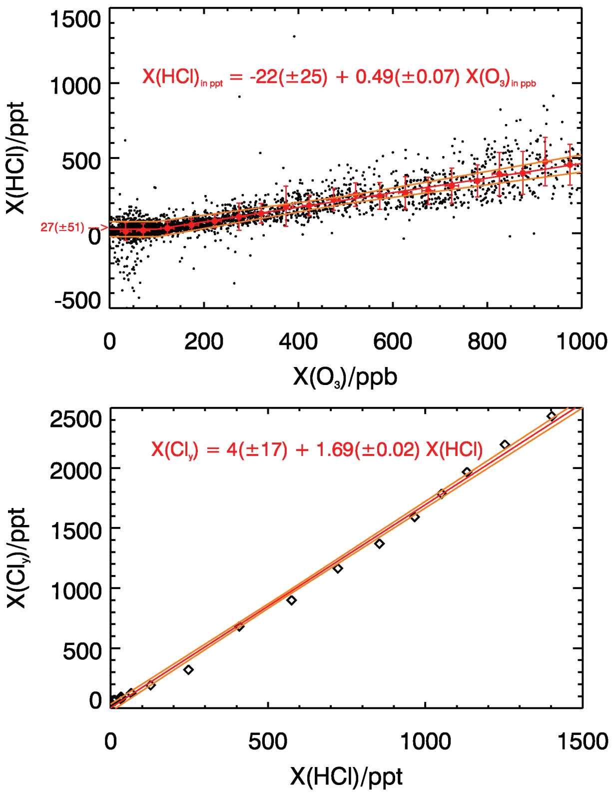

Fig. 1. Correlations used to estimate Cl_y from O_3. **(a)** Correlation of HCl vs. O_3 based on ACE-FTS satellite observations (Version 2.2-update) in the latitude band 30° N–30° S between November 2004 and February 2006 (black symbols) averaged in 50 ppb O_3 bins (red symbols with 1σ-error bars for HCl and O_3). **(b)** Correlation of Cl_y vs. HCl based on the tropical (30° N–30° S) chlorine inventory (based on ACE-FTS measurements of a large number of inorganic and organic chlorine containing trace gases from February 2004–January 2005) recently published by Nassar et al. (2006).

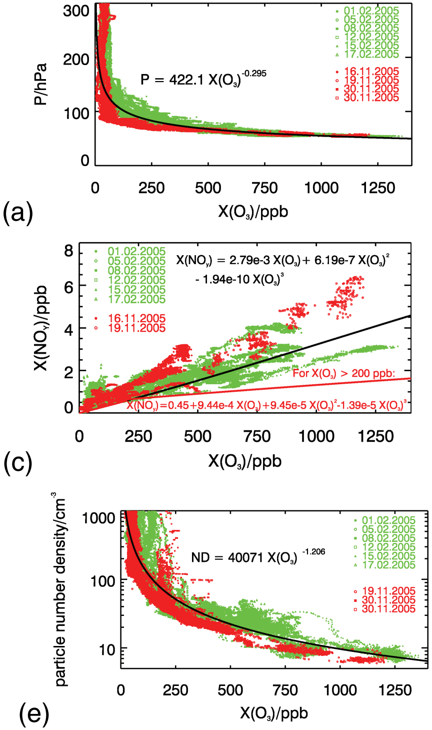

Fig. 2. Relationship of **(a)** pressure, **(b)** temperature, **(c)** [NO$_y$], **(d)** total water and **(e)** aerosol number densities with O$_3$ observed during TROCCINOX and SCOUT-O$_3$, used to initialise the CLaMS_ST simulation to estimate typical noontime Cl activation. Best fit relationships (lines) were determined for the measured data except for [NO$_y$] in panel (c), where correlations from Michelson et al. (1998) are shown.

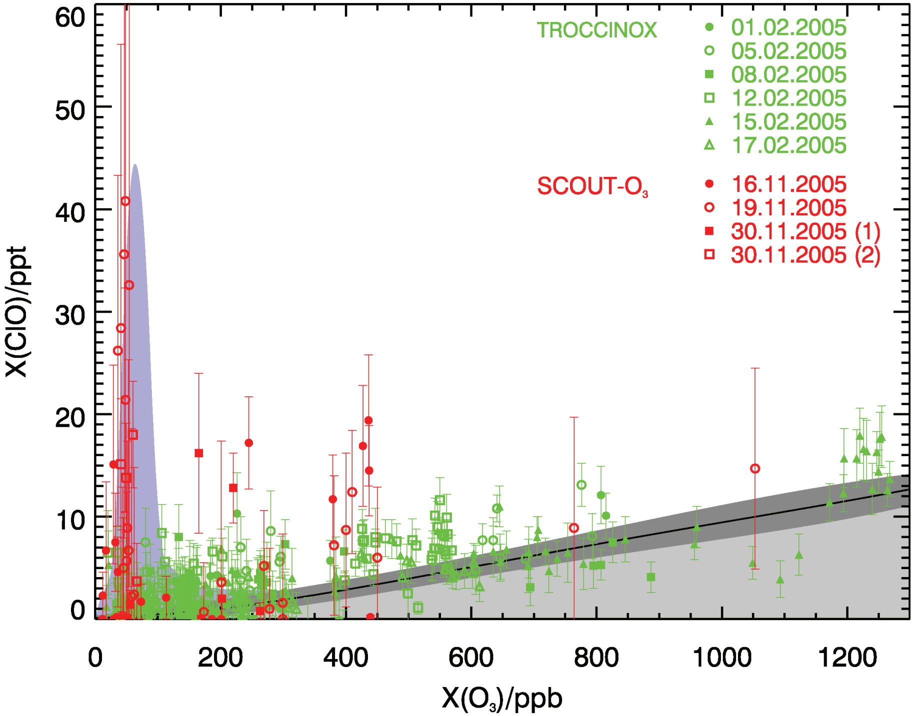

Fig. 3. Relation between ClO and Ozone in the tropical UTLS. Symbols with error bars represent HALOX measurements made during TROCCINOX and SCOUT-O_3 field campaigns. The black line shows ClO mixing ratios expected at local noon based on CLaMS_ST box-model simulations without heterogeneous reactions included; the range of values due to uncertainties in the Cl_y–O_3 correlation and temperature is shown in dark grey. ClO mixing ratios observed at times significantly before or after local noon are expected to fall below this line as indicated by the light grey area. Blue shading indicates the range of ClO predicted with heterogeneous chemistry included; the upper limit is defined by the simulation with highest Cl_y (Fig. 1) and lowest temperatures (Fig. 2b).

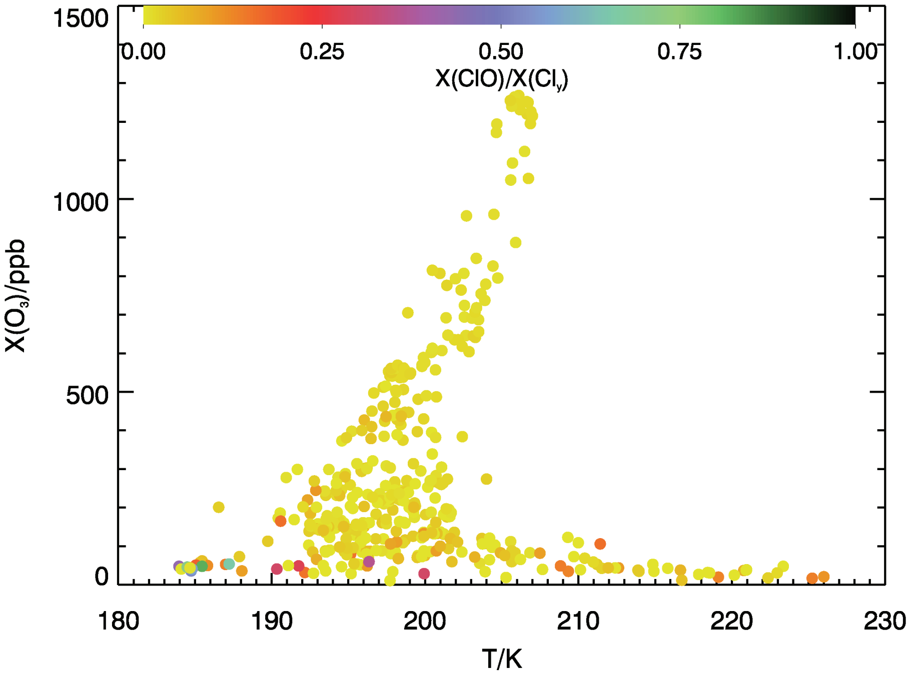

Fig. 4. Dependence of ClO/Cl$_y$ on temperature and O$_3$ at time of observation.

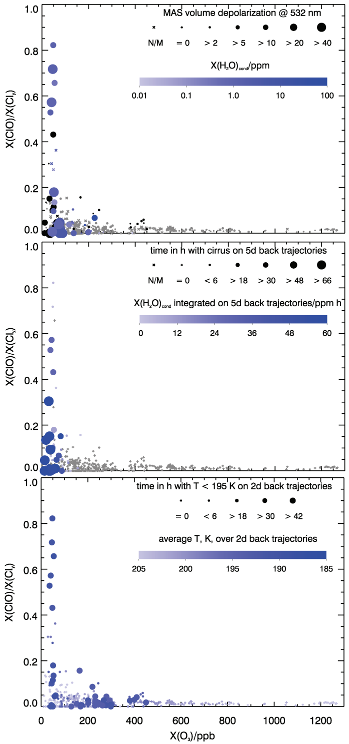

Fig. 5. ClO/Cl$_y$ ratios as a function of O$_3$ mixing ratio and characterization of the "heterogeneous chemistry potential": **(a)** ice water content (colour code; grey: [H$_2$O]$_{cond}$=0, black: no data) and volume depolarisation (symbol size; N/M: not measured) as proxies for cirrus particles; **(b)** integrated ice water content (colour code) and time with ice present (symbol size; N/M: not measured) simulated on 5 day back trajectories to estimate the extent of cirrus occurrence preceding the flights; **(c)** mean ECMWF temperatures for 2 day back trajectories (colour code) and time at $T < 195$ K.

Title Page
Abstract
Introduction
Conclusions
References
Tables
Figures
◀◀
▶▶
◀
▶
Back
Close
Full Screen / Esc
Printer-friendly Version
Interactive Discussion

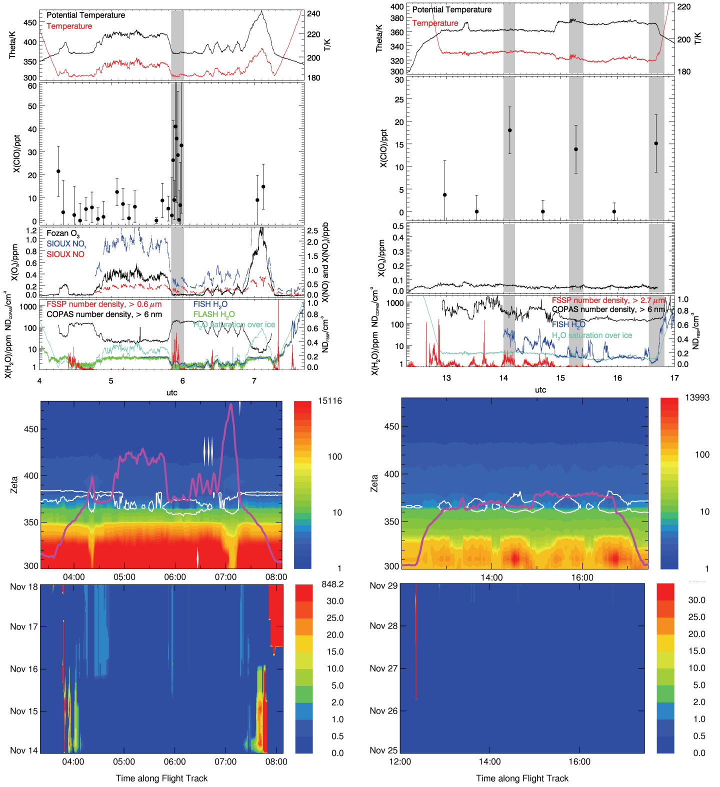

Fig. 6. Case studies for the SCOUT-O$_3$ flights on 19 (left) and 30 November 2005 (right) from Darwin. **Upper panels**: observations made during the flights (see text for details). **Middle panels**: CLaMS_CTM simulations of IWC vs. altitude along the Geophysica flight track (magenta line). White contours indicate the predicted occurrence of cirrus clouds. **Lower panels:** CLaMS_CTM simulations of IWC along 5-day-back-trajectories ending on the Geophysica flight track.

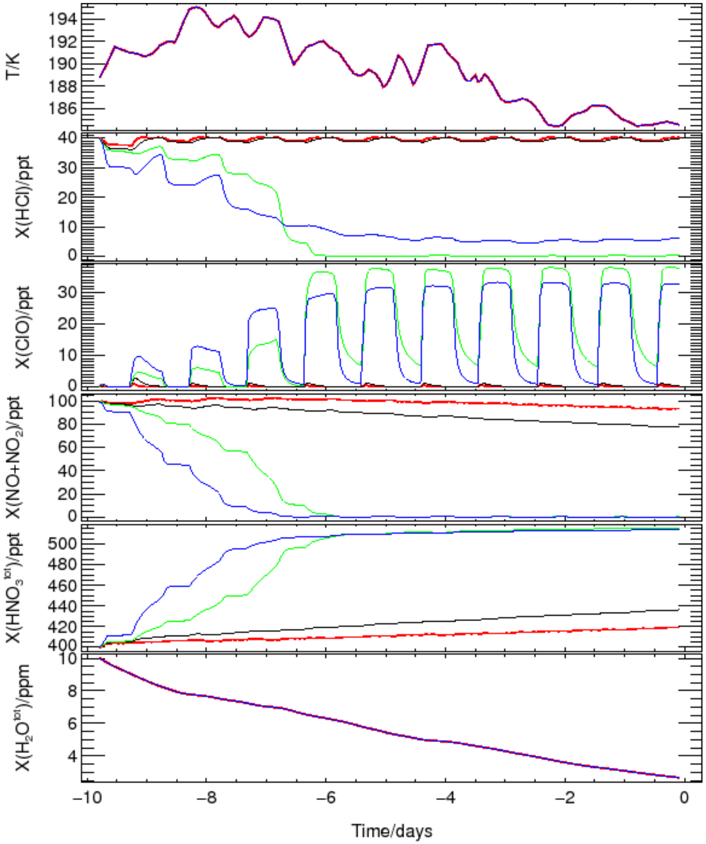

Fig. 7. CLaMS_BT simulation results for the flight on 19 November 2005 for various parameters along one chosen back-trajectory in the time window where chlorine activation was observed by HALOX for different initialisations: red: 1 ppt Br_y/50 ppb O_3; black: 1 ppt Br_y/125 ppb O_3; green: 1 ppt Br_y/200 ppb O_3; blue: 5 ppt Br_y/125 ppb O_3.

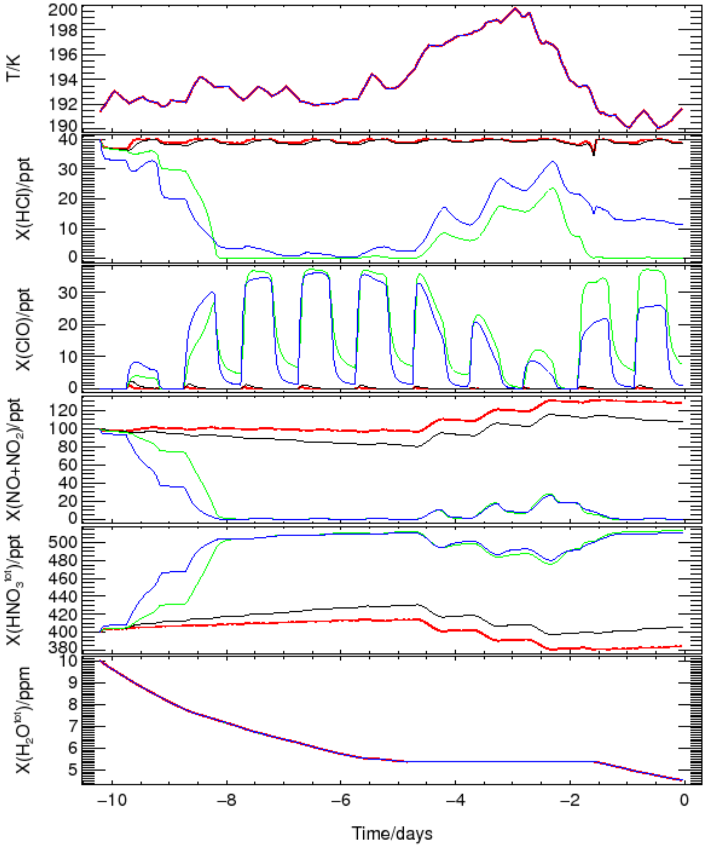

Fig. 8. CLaMS_BT simulation results for the flight on 30 November 2005 for various parameters along one chosen back-trajectory in the time window where chlorine activation was observed by HALOX for different initialisations: red: 1 ppt Br_y/50 ppb O_3; black: 1 ppt Br_y/125 ppb O_3; green: 1 ppt Br_y/200 ppb O_3; blue: 5 ppt Br_y/125 ppb O_3.

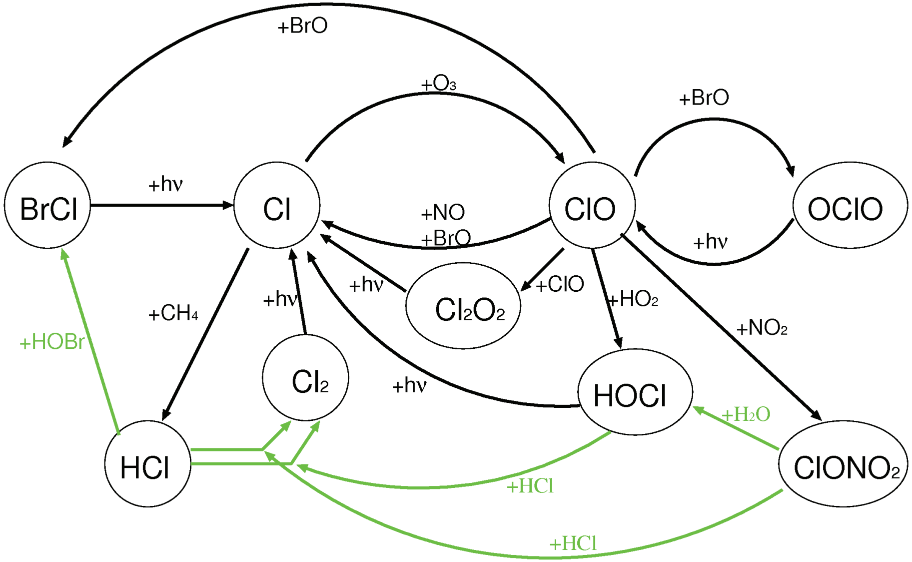

Fig. 9. Schematic of the chemical reaction system governing chlorine partitioning in ClaMS.

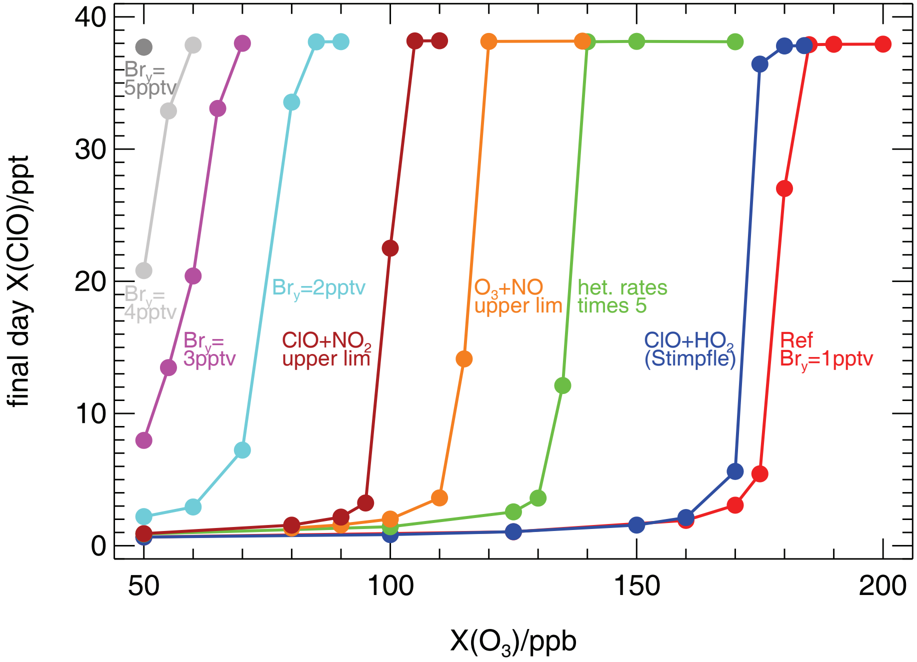

Fig. 10. Sensitivity of final day ClO in the CLaMS_BT simulation results for the flight on 19 November 2005 (Fig. 7) to Ozone mixing ratio for various input parameterisations. The changes made to the reference parameterisation (red) are indicated in the graph and are cumulative from right to left.